Organically Templated Open-Framework Vanadium Phosphates: Hydrothermal Synthesis, Structure, and Magnetic Properties of $H_3N(CH_2)_3NH_3[(VO)_3(OH)_2(H_2O)_2(PO_4)_2]$

Victoria Soghomonian,[1a,b] Qin Chen,[1b]
Robert C. Haushalter,*[1a] Jon Zubieta,*[1b]
Charles J. O'Connor,[1c] and Young-Sook Lee[1c]

NEC Research Institute, 4 Independence Way
Princeton, New Jersey 08540
Department of Chemistry, Syracuse University
Syracuse, New York 13244
Department of Chemistry, University of New Orleans
New Orleans, Louisiana 70148

Open-framework and microporous solids comprise a fascinating class of materials with most of their interesting properties resulting from the fact that the frameworks divide space into occupied and unoccupied regions with dimensions on the order of small molecules. The most well-known use derived from this partitioning of space is the ability of these microporous solids to sorb small molecules into these voids. The naturally occurring and synthetic microporous solids, most of which are silicoaluminates[2] and aluminophosphates,[3] are closed shell diamagnetic solids. Recently, however, some progress has been made toward preparing organically templated microporous solids containing transition elements as stoichiometric framework constituents in the molybdenum phosphate[4] system. Open-framework oxides like these could have useful properties, derived from the enhanced catalytic activity combined with shape-selective absorptivities and the possibility of generating vacant coordination sites on the transition element component, when compared to the Si- and Al-containing materials. We recently extended the synthesis of organically templated three-dimensional (3-D) open-framework transition-metal oxide to include materials in the vanadium phosphate system.[5–7] Examples include $(H_3N(CH_2)_3NH_3)K[(VO)_3(PO_4)_3]$,[5] chiral intertwined double helices in $[(CH_3)_2NH_2]K_4[V_{10}O_{10}(H_2O)_2(OH)_4(PO_4)_7]·4H_2O$[6] and very large ethylenediamine filled tunnels in $(NH_3(CH_2)_2NH_3)_{2.5}[V(H_2O)_2(VO)_8(OH)_4(HPO_4)_4(PO_4)_4]·2H_2O$.[7] We report here the synthesis and structural characterization of $(NH_3(CH_2)_3NH_3)[(VO)_3(OH)_2(H_2O)_2(PO_4)_2]$ (1), a new
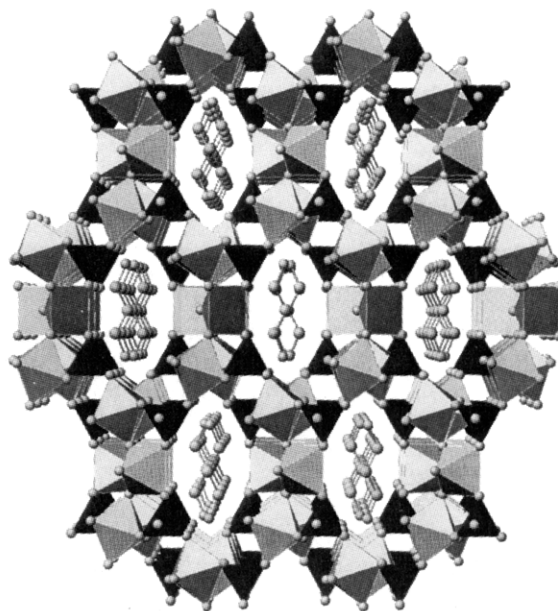

Figure 1. View of the unit cell contents projected down [100] parallel to the propanediammonium (PDA) filled tunnels. The V are represented by the octahedra and square pyramids while the phosphate groups are drawn as tetrahedra.

organically templated, open-framework 3-D vanadium phosphate which displays interesting and complicated magnetic properties.

The hydrothermal reaction of $H_3PO_4:VCl_4:1,3$-diaminopropane:H_2O in the mole ratio of 8.21:1:12.02:1115 at 200 °C for 48 h gives an 86% yield (based on VCl_4) of single phase (1) as dark blue plates which crystallize in the orthorhombic space group *Pnma*.[8] Structurally complicated phosphate 1, like other of our organically templated V–P–O materials that self-assemble from structurally simple precursors,[5–7,9] contains an anionic 3-D framework with the organic cations residing in tunnels within the framework. A view of the unit cell contents projected down [100] parallel to the propanediammonium (PDA) filled tunnels is shown in Figure 1. The basic structural motif is built up from vanadium trimers and a single crystallographically unique phosphate group that create the anionic framework encapsulating the organic templates. The $-NH_3^+$ groups of the PDA cation are strongly hydrogen bonded to the framework[10] with the N making contact to four framework O atoms at 2.85(1), 2.86(1), 2.91(1), and 2.98(1) Å. The trimers (Figure 2), which lie on the crystallographic mirror planes that are perpendicular to the *b* axis at $b = 1/4$ and $3/4$, consist of two distorted VO_6 octahedra on the ends of the trimer and a square pyramidal VO_5 located in the center. The two octahedra have short vanadyl (V=O) groups (V1–O5 = 1.601(8) Å) *trans* to aquo ligands[10] that have long V1–O7 bonds of 2.363(5) Å. Valence sum calculations confirm that all of the V are present as V^{4+}.[11] The central square

(1) (a) NEC Research Institute; (b) Syracuse University; (c) University of New Orleans.

(2) Occelli, M. L.; Robson, H. E. *Zeolite Synthesis*; American Chemical Society: Washington, DC, 1989. Breck, D. W. *Zeolite Molecular Sieves*; Krieger: Malabar, FL, 1974; Vaughan, D. E. W. In *ZEOLITES: Facts, Figures, Future*; Jacobs, P. A., van Santen, R. A., Eds.; Elsevier: Amsterdam, 1989; pp 95–116. Meier, W. M.; Olson, D. H. *Atlas of Zeolite Structure Types*; Butterworth: London, 1987; Barrer, R. M., Eds.; *Hydrothermal Chemistry of Zeolites*; Academic Press: New York, 1982.

(3) Szostak, R. *Molecular Sieves Principles of Synthesis and Identification*; Van Nostrand Reinhold: New York, 1989. Meier, W. M.; Olson, D. H. *Atlas of Zeolite Structure Types*; Butterworth: London, 1987. Occelli, M. L.; Robson, H. E. *Zeolite Synthesis*; American Chemical Society: Washington, D.C., 1989; Chapter 23.

(4) Review: Haushalter, R. C., Mundi, L. A. *Chem. Mater.* **1992**, *4*, 31.

(5) Soghomonian, V.; Haushalter, R. C.; Chen, Q.; Zubieta, J. *Chem. Mater.*, in press.

(6) Soghomonian, V.; Haushalter, R. C.; Chen, Q.; Zubieta, J.; O'Connor, C. J. *Science* **1993**, *259*, 1596.

(7) Soghomonian, V.; Haushalter, R. C.; Chen, Q.; Zubieta, Z.; O'Connor, C. J. *Angew. Chem., Int. Ed. Engl.* **1993**, *32*, 610.

(8) Crystal data for 1: orthorhombic, space group *Pnma* with $a = 10.507(2)$, $b = 17.136(3)$, and $c = 8.451(2)$ Å, $V = 1521.6(8)$ Å³, $Z = 4$ and $R(R_w) = 0.0363(0.0444)$ for 904 reflections and 105 refined parameters.

(9) Soghomonian, V.; Haushalter, R. C.; Zubieta, J., unpublished results.

(10) Thermogravimetric analysis under N_2 shows a weight loss of 8% at 325 °C assigned to the loss of water and a 13% loss at 400 °C attributed to the loss of the diaminopropane. The calculated weight losses are 7% and 14% respectively.

(11) Brown, I. D. In *Structure and Bonding in Crystals*; O'Keefe, M., Navrotsky, A., Eds.; Academic Press: New York, 1981; Vol. II, pp 1–30.
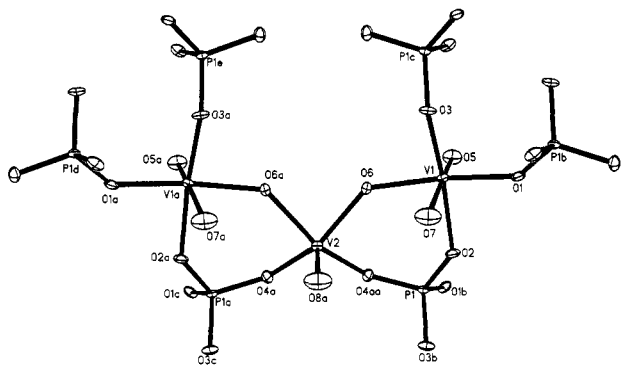
Figure 2. V^{4+} trimers which lie on the crystallographic mirror planes that are perpendicular to the b axis at $b = 1/4$ and $3/4$. There are two distorted VO_6 octahedra on the ends of the trimer and a square pyramidal VO_5 in the center.
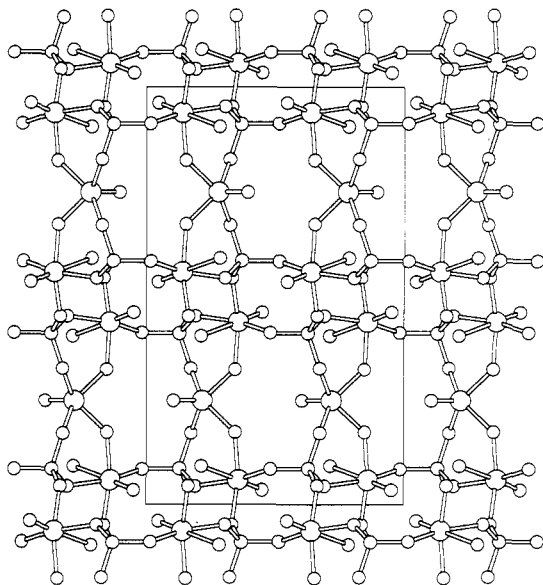

Figure 3. View of the unit cell contents projected down [001].

Figure 4. Magnetic susceptibility χ (M/H) (emu mol^{-1}) as a function of temperature (K) for 1. The numbers on some data points are the applied measuring fields in gauss (a and b) or kilogauss (c). In (d), the sample was cooled in a 10-G field and measured in a 100-G field.

is bridged to the octahedra via μ^2-OH groups with V1-OH = 1.980(5) Å and V2-OH = 1.968(5) Å (Figure 2). The trimers are connected by the phosphate groups into stacks, which are reminiscent of ladders with the square-pyramidal vanadium centers as the rungs, that run parallel to [100] as shown in projection down [001] in Figure 3. If only covalent bonds are considered, then the trimers are effectively isolated from one another by the PO_4 groups and the nearest V···V interactions are via V-O-P-O-V linkages. But closer inspection of the structure shows the presence of very short non-bonded V=O···O=V interactions, of only 2.81(1) Å, which appear in projection in Figure 3 as being located at the origin as well as at the edge and face centers of the cell.

Phosphate 1 displays very interesting and unusual magnetic properties. At room temperature the V atoms display an effective magnetic moment near 3 μ_B consistent with three noninteracting $S = 1/2$ V^{4+} centers. As the sample is cooled, deviations from Curie–Weiss behavior become apparent below ca. 50 K and the magnetic moment begins to decrease. Studies of the susceptibility of 1 as a function of temperature and applied measuring field are shown in Figure 4. The decrease in χ below 50 K manifests itself in a broad local maximum near ca. 6.5 K, as shown in Figure 4B, suggestive of short-range antiferromagnetic ordering possibly attributable to the antiferromagnetic
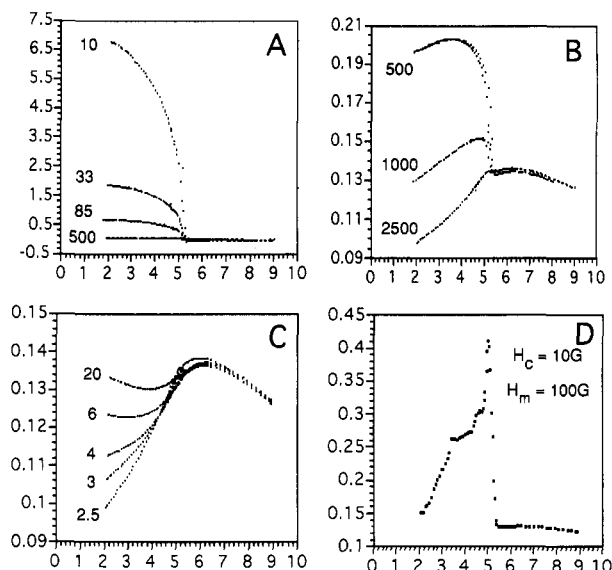
coupling of the spins between the trimers. Near 5.2 K the material undergoes an ordering into a weakly ferromagnetic state. The transition is extremely sensitive to the magnitude of the measuring field and χ below the ferromagnetic transition is initially suppressed as the field is increased as shown in Figure 4A,B, but this trend is reversed as the measuring field is increased further. As the measuring field is increased above 2.5 kG, the lower temperature susceptibility once again begins to increase (Figure 4C) and continues increasing at the highest fields (ca. 20 kG) we studied. When samples are cooled in cooling fields near zero and then measured upon warming in small applied fields (Figure 4D), there are indications of a still more complicated magnetic phase diagram. An interesting question is the nature of the longer range interactions developing, even though the magnetically active trimers are separated from one another by the insulating phosphate groups. As mentioned above, the vanadyl oxygen atoms of the octahedral VO_6 at both end of the trimer contact the V=O groups of two adjacent trimers at 2.81 Å which is essentially the van der Waals radius for O. Polarization of the π electrons of the V=O groups could provide a possible exchange pathway for the longer range interactions. However, until the complicated interactions can be successfully modeled, these hypotheses remain speculative.

The incorporation of the large PDA cations into a vanadium phosphate material extends the open-framework transition element phosphates into a large pore size range. Additional experiments involving template removal to access the potential internal micropore volume, as well as additional magnetic measurements, are currently under way.